DELPHI Collaboration

DELPHI 2001-144 PHYS 915
17 DECEMBER, 2001

Study of the photon structure function F_2^γ in the reaction $e^+e^- \to e^+e^- + hadrons$ at LEP1

I. Tyapkin, N. Zimin, A. Zinchenko

Abstract

The photon structure function F_2^γ has been studied at average Q^2 values of 5.2 GeV^2, 12.7 GeV^2 and 28.5 GeV^2. The data correspond to the integrated luminosity of 72 pb^{-1}, collected by the DELPHI detector during the 1994-1995 LEP runs. Experimental distributions are compared with predictions of different models. The contribution from the resolved photons has been included in the analysis. The F_2^γ reconstructed from the data is compared with theoretical expectations based on different models. A result for Q^2 evolution of the photon structure function has been obtained.

1 Introduction

The photon structure function has been measured at PETRA and PEP [1, 2, 3, 4, 5, 6] and more recently at TRISTAN [7, 8] and LEP [9, 10, 11, 12, 13, 14, 15, 16, 17, 18] in the reaction $e^+e^- \rightarrow e^+e^-X$, where X is a multihadronic system and one of the scattered leptons is observed at a large scattering angle (tagging condition) while the other, remaining at a small angle, is undetected (anti-tagging condition). This reaction can be described as a deep inelastic $e\gamma$ scattering (DIS), where γ is almost a real photon. The corresponding cross-section is usually expressed in terms of the photon structure functions $F_2^\gamma(x,Q^2)$ and $F_L(x,Q^2)$:

$$\frac{d\sigma}{dE_{tag}d\cos\left(\theta_{tag}\right)} = \frac{4\pi\alpha^2 E_{tag}}{Q^4 y}\left[(1+(1-y)^2)F_2^\gamma(x,Q^2) - y^2 F_L(x,Q^2)\right]. \qquad (1)$$

Here, E_{tag} and θ_{tag} are the energy and polar angle of the tagged lepton, Q^2=$4E_{tag}E_{beam}\sin^2(\theta_{tag}/2)$, x=$Q^2/(Q^2+W^2+P^2)$, y=1-$(E_{tag}/E_{beam})\cos^2\theta_{tag}$, W is the invariant mass of the hadronic system and and P^2 is the negative four-momentum squared for the virtual photon emitted from the anti-tagged electron. Anti-tagging conditions ensures that P^2 is much smaller than Q^2. But experimentally the influence of the real photon virtuality (P^2) is not negligible and photon structure function should be treated as a function of this value i.e. $F_2^\gamma(x,Q^2,P^2)$. Due to small values of y in the experimentally accessible region, an influence of F_L on the cross-section is small (about few percent) and may be taken into account in the simplified way given an additional uncertainty of these measurements.

The photon structure function can be calculated from the diagrams in Fig.1. The contributions from the component Fig.1(a) and (c) can be evaluated in the frame of perturbative quantum chromodynamics (QCD). The contribution from the non-perturbative

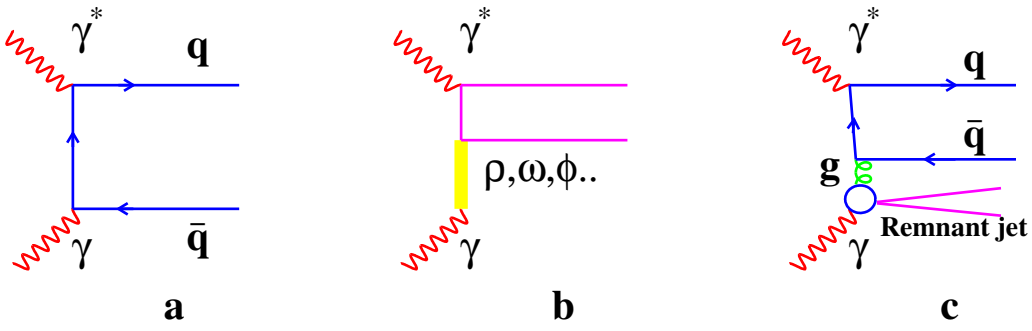

Figure 1: The point-like (a), the hadron-like (b) and RPC (c) contributions to F_2^γ.

component (Fig.1b VDM-like) is significant and can not be calculated in the frame of perturbative theory. Several authors [19, 20, 21, 22, 23] tried to calculate corresponding F_2^γ but the difference in their results, originated from the treatment of hadronic part and choice of boundary conditions for the perturbative equations is rather large. In 1996 OPAL [24] and DELPHI [25] have stressed the importance of a proper description of the hadronic state by models used in the analysis. It has been shown, that a poor description

of the hadronic system produced in $\gamma\gamma^*$ interactions can be due to a missing component in the models. Moreover, problems in the description of the hadronic system lead to a distortion of a correlation between x_{vis} and x_{true} given by the model. Both factors mentioned above can result in a significant bias in an estimation of the structure function. All studies before 1996 were based on the generators included two components, the QPM-like describing the perturbative part (Fig. 1a), and the VDM-like for the hadron-like part (Fig. 1b). As shown by the DELPHI collaboration in [25] this approach gives a poor description of the final state and, as a result, leads to significant bias in the structure function estimation. The solution proposed by the DELPHI collaboration consists in introducing the hard scattering process (Fig.1c) in the description of the process (RPC-resolved photon contribution). Here the partonic densities of the photon are used to describe interaction between highly virtual photon and one of the partons of the resolved photon. Such a modification significantly improves the agreement with experimental data. This leads to a more correct description of the final state topology which is crucial for the interpretation of the results. This approach can be realised by making use of the TWOGAM [26] and PHOJET [27] generators. Recently, the general-purpose generators PYTHIA [28] and HERWIG [29] have been also adopted to DIS study. All new generators use the parton density functions of the photon which are obtained under recent theoretical assumptions but require additional input data, namely, experimental measurements of the photon structure function. Influence of the parton density functions on the results given by TWOGAM and PHOJET is much smaller because these generators use it only for RPC. From this point of view, new measurements will definitely affect theoretical predictions.

That is why new studies are needed to improve an understanding of the real photon which will be increasingly important in $\gamma\gamma$ and γp interactions at higher energies.

2 Event selection

The detailed description of the DELPHI detector can be found in [30]. The components of the detector relevant to the analysis of $\gamma\gamma$ events have been described in our previous papers [10], [31]. Data used in this analysis were collected with the DELPHI detector at the LEP e^+e^- collider during the 1994-1995 runs. The range of centre-of-mass energies is from 88.6 GeV to 94.6 GeV. The tagged particles were detected by the DELPHI luminometer STIC.

The following criteria were used to select a pure sample of $\gamma\gamma^*$ events:

1. The energy deposited by the tagged electron (or positron) in the detector must be greater than $0.4 * E_{beam}$ (tagging requirement);

2. No additional clusters with energy exceeding $0.3 * E_{beam}$ must be observed anywhere in the forward calorimeters (anti-tagging requirement);

3. The track multiplicity is 3 or more. This includes only tracks with momenta greater than 0.25 GeV/c with a polar angle between 20° and 160° and an impact parameter of less than 4 cm in the radial direction and less than 8 cm along the beam (hadronic final state selection);

4. The visible invariant mass of the hadronic system must be greater than 2.5 GeV;

5. The vector sum of transverse momenta of all particles, including tagged particle, normalized to E_{beam} must be less than 0.12;

6. The absolute value of the sum of longitudinal momenta of particles normalised to E_{beam} must be greater than 0.6.

In this analysis all the DELPHI calorimeters are used for event reconstruction. It strengthens the correlation between x_{true} and $x_{visible}$. Calorimetric clusters were accepted if their energy deposition exceeded 0.5 GeV in the forward or barrel electromagnetic calorimeters, 1.0 GeV in the hadron calorimeter and 1.5 GeV in the luminometer.

Finally, a total of 3159 events were selected. The main source of background is Z^0 hadronic decays and their contribution was estimated as 1.1 pb. The background from $\gamma\gamma^* \to \tau\tau$ and $\gamma\gamma^* \to e^+e^-$ interactions was estimated from a simulation as 0.6 pb and 0.2 pb respectively. The contamination from other sources of background was found to be much lower. After subtraction of the background the visible cross-section of the investigated process was estimated as being 41.9 pb. This sample was used as a basis of this study, some variations of the selection criteria were allowed to study the systematics. The average Q^2 for the selected events is about 12.7 GeV^2. The trigger efficiency was studied and found to be of the order of 98 $\pm$ 1%.

3 Event generators

Two generators were used to produce simulated samples. A two-photon event generator TWOGAM [26] was successfully tested in previous DELPHI studies. It is based on the exact helisity decomposition of the process. The total cross-section is described by the sum of three parts: point-like (QPM), resolved photon contribution (RPC) and soft hadronic (VDM). For the point-like part the exact differential cross-sections [32] are used. The quark masses are taken to be 0.3 GeV for u and d quarks, 0.5 GeV for s and 1.6 GeV^2 for c quarks. For the single or double resolved perturbative part (RPC) the lowest order cross-sections are used. Only the transverse-transverse part of the luminosity function is used in this case.

There is no initial or final state parton showering. Strings are formed following the colour flow of the sub-processes. The remnant of a quark is an antiquark (and vice versa), and the remnant of a gluon is a $q\bar{q}$ pair. The produced system is fragmented as a string by JETSET 7.4.
A transverse momentum cutoff, p_t^{cut}=1.8 GeV, is applied to the partons of the resolved photons to separate soft from hard processes. In this analysis the GVDM structure function multiplied by the factor (1-x_{true}) for the soft hadronic part was used. TWOGAM treats exactly the kinematics of the scattered electron and positron, and uses exact (unfactorised) expressions for the two photon luminosity function. New version of TWOGAM (2.04) was used in this analysis.

Second Monte Carlo event generator PHOJET [27] (version 1.12). The generator includes the exact photon flux simulation for photon-photon processes in lepton-lepton collisions. The ideas and methods used in the program are based mainly on the Dual Parton Model (DPM). In order to combine the DPM on soft processes with the predictive power of perturbative QCD, the event generator is formulated as a two-component model (soft and hard components). On the basis of the optical theorem, Regge phenomenology is

used to parametrise the total and elastic cross-sections as well as a series of partial inelastic cross-sections. In order to conserve s-channel unitarity, Gribov's Reggeon calculus is applied. Consequently, the model predicts so-called "multiple parton interactions" in one event. Since the unitarization of soft and hard processes is treated in unified way, multiple soft and hard interactions may be generated in one event. Hard scattering processes are simulated using lowest-order perturbative QCD. Initial state and final state parton showers are generated in leading-log approximation. Some coherence effects (angular ordering in the emissions) are taken into account. For the fragmentation of the parton configurations, the JETSET program is used. Program can run only in the invariant mass region above 5 GeV.

4 Comparison of experimental and simulated data

As it was mentioned in Section 1 a good modelling is necessary for an accurate measurement of F_2^γ. Due to finite detector resolution and acceptance, the final state topology defines the correlation between x_{true} and $x_{visible}$ and the acceptance factor is crucial for the transition from x_{true} distribution to F_2^γ. Each component of the model has different x_{true}-$x_{visible}$ correlation and the acceptance factor. Therefore, not only the final state topology for each component but also the cross-section of each component should be properly simulated. To check available models the inclusive and global event distributions should be compared for data and Monte Carlo predictions. Special attention should be paid to the distributions which are not strongly correlated with x_{true} and which cannot be corrected by tuning F_2^γ.

Both generators mentioned above were used to describe experimental distributions. The Q^2, E_{tag}/E_{beam} and W_{vis} spectra are shown in Fig.2. One can see that TWOGAM overestimates and PHOJET underestimates the total visible cross-section. The main difference in TWOGAM comes from the low- W region. While PHOJET is suppressed in a wide W region. A detailed analysis of these models shows that they differ mostly in their point-like part due to the $p_t = 2.5$ GeV cut applied in PHOJET to partons in the final state. As examples of the distributions weakly correlated with x_{true}, spectra of E_{tot} and N_{tot} are shown in Fig.3(a-b). The distributions directly reflecting the final state topology are shown in Figs.3c,4. The hadronic energy out of tagged particle plain is one of the observables reflecting topology of the final state (Fig.3c). The energy flow versus pseudorapidity, defined as $\eta = -\ln(\tan(\theta/2))$, where θ is the polar angle of final state particles, is shown in different Q^2 bins. A reasonable agreement between data and the TWOGAM Monte Carlo prediction is found in all Q^2 ranges. Finally, x_{vis} distributions for the same Q^2 ranges are shown in Fig.5. From Figs.2-5 we can conclude that TWOGAM gives the better agreement with the data.

The HERWIG and PYTHIA generators with SaS and GRV parameterisations fail to reproduce data in this Q^2 region, and give a rather poor description of variables defined by the event topology. Its why they are not used in this analysis.

5 Extraction of the structure function

The usual way of F_2^γ extraction from data is to use the method of regularized unfolding (for example, Blobel's unfolding program [36]). In this method a Monte Carlo simulation

is used to find a response matrix for a transition from x_{true} to $x_{visible}$ which includes the effect of limited detector resolution ($W_{visible}$ is lower than W_{true}). Then a regularized unfolding obtains the x_{true} distribution for the data. As a last step F_2^γ is determined by reweighting the input structure function of the Monte Carlo according to the ratio of the unfolded x_{true} distribution to the x_{true} distribution in the Monte Carlo. This step takes into account the efficiency effect (not all the events can be detected, triggered or selected by the selection criteria). Thus, the unfolding method does not take into account a difference in the correlations for each of the components in the model. The reweighting factor is also determined by unfolding for a sum of the components in the model without taking into account their differences. These two factors make usual unfolding procedure not adequate to the task. A priori some of the components can be correctly simulated in the generator but some others should be fitted to the data. Only on a basis of statistical comparison of many of reweighted simulated and experimental distributions one can decide which components should be modified.

First of all, x_{true} divided on the N_{bin} bins. The correction factor A_{ij} are introduced for each bin of x^i_{true} (here i running form 1 to N_{bin}) and each model component (the QPM j=1, VDM j=2 and RPC j=3). These factors A_{ij} are the free parameters for the MINUIT fit of $x_{visible}$ Monte Carlo distribution to the date one. Fitting procedure were repeated many times with different sets of A_{ij}. In this analysis only four correction factors A_{1k}, A_{2l}, A_{3m} and A_{4n} (where k,l,m,n can be any number from 1 to 3) are used in each fit. Thus, the total of 81 fits with different combinations ofA_{ij} are performed for four x_{true} bins analysis. As a result of each fit, we have an estimation of structure function with corresponding reweighted by A_{ij} simulated distributions. Most of the fits give the statistically acceptable quality and only on the basis of the analysis of many additional distributions one can make a choice between these fits. The statistical analysis of these distributions gives χ^2 which is then considered as a weight factor for F_2^γ averaging. Thus, weighted average of all fits results gives the estimation for F_2^γ. The difference in each x bin for different fits represents the systematic error due to the choice of the model or combinations of the models for the fit (modelling systematics). Even the statistical error for each x bin depends on the choice of the model due to different efficiencies of event selection for each model.

The test of the fitting procedure has been done. The sample simulated by the PHOJET program was used to extract the structure function used in TWOGAM. The results of this test together with the test of Blobel's unfolding program are shown in Fig.5(a,b). Solid lines are the structure function used in the TWOGAM. Open circles correspond to the fit with the Monte Carlo sample treated as a sum of three components. Black dots in Fig.5a better represent structure function and correspond to the complete MINUIT fitting procedure described above. For comparison the results of unfolding procedure are presented in Fig.5b. As expected, the unfolding procedure leads to some bias and underestimates the errors.

The value of F_L^γ was estimated by TWOGAM and then subtracted from the result. The same generator have been used to estimate correction factors for each x-bin which taking into account the non-zero virtuality of the target photon in the experiment. All results then corrected on these factors to get F_2^γ for the P^2=0. Bins in x are chosen to have compatible statistics in each of them and correlations between bins to be not too high. The correlation matrix for each of the presented results was checked. The maximum correlation between bins is found to be below 0.35.

$< Q^2 >$ GeV^2	x range	F_2^γ/α	Stat. err.	Mod. err.	Det. err.	Back. err.	Tot. Sys. err.	Tot. err.
5.2	0.001-0.02	0.283	0.011	0.010	0.023	0.005	0.026	0.028
	0.02-0.1	0.203	0.014	0.023	0.007	0.002	0.024	0.028
	0.1-0.5	0.212	0.020	0.030	0.013	0.004	0.033	0.039
12.7	0.001-0.02	0.446	0.015	0.010	0.025	0.005	0.027	0.031
	0.02-0.1	0.317	0.018	0.008	0.010	0.003	0.013	0.022
	0.1-0.3	0.286	0.034	0.010	0.010	0.005	0.015	0.037
	0.3-0.8	0.362	0.015	0.020	0.020	0.006	0.029	0.033
28.5	0.02-0.1	0.413	0.030	0.030	0.018	0.004	0.035	0.043
	0.1-0.3	0.346	0.015	0.033	0.008	0.002	0.034	0.037
	0.3-0.8	0.488	0.037	0.030	0.011	0.006	0.033	0.050

Table 1. Summary for the F_2^γ measurements in three bins of Q^2.

In Fig. 7 the measurements presented in Table 1 are illustrated. The first error is the statistical one (Stat. err.) which in this approach also depends on the model, and in some sense, carries some systematic uncertainty. The model dependent shift in F_2^γ measured in each x bin was interpreted as a modelling systematics (Mod. err.) and is shown in the Table 1-3 in the fifth column. Fit brings to the good agreement between most of distributions in data and Monte Carlo but it does not help in improving an agreement in the energy flow distribution. It is why systematic error due to the uncertainty in the energy flow description was studied separately. As it is seen from the Monte Carlo study correction to the E_{flow} leads to the shift of the extracted value of F_2^γ. This shift interpreted as a systematic error (E_{flow}). The shift of unfolding results due to variation in the selection criteria (W_{min}, N_{min}^{trk}...), thresholds for detection of neutral particles by the calorimeters and uncertainty in the measurement of invariant mass was interpreted as a detector dependent systematic error (Det. err.). The background systematic error (Back. err.) reflects an uncertainty in the knowledge of the background and was estimated from $Z^0\gamma$ hadronic and $\gamma\gamma \to \tau\tau$ Monte Carlo as an uncertainty with which we are able to describe the corresponding data samples. Certainly, there are some other sources of systematics in the measurements, but their influence is estimated as much lower.

To study the Q^2 evolution of F_2^γ, the data were fitted in the same three $< Q^2 >$ bins in the x intervals 0.001-0.02, 0.001-0.1 and 0.3-0.8. The results are shown in Table 2 and in Fig.8.

Sample	$< Q^2 >$=5.2 GeV^2	$< Q^2 >$=12.7 GeV^2	$< Q^2 >$=28.5 GeV^2
0.001-0.02	0.283±0.011±0.026	0.446±0.015±0.027	
0.001-0.1	0.219±0.010±0.022	0.331±0.015±0.018	0.413±0.060±0.045
0.3-0.8		0.362±0.015±0.029	0.488±0.037±0.033

Table 2. Results for F_2^γ in three bins of Q^2.

The first errors are statistical and the second systematic. The systematic error includes the same components as in Table 1.

6 Conclusions

The photon structure function F_2^γ has been measured at LEP with the DELPHI detector. The measurements are done in Q^2 interval from 3 to 60 GeV^2 and in the x range from 0.001 to 0.8.

Both Monte Carlo generators used in this analysis are based on the three component description of $\gamma\gamma^*$ interaction and give reasonable description of the process.

In the lowest x bin the data are slightly above predictions of all models (GRV, SaS) and TWOGAM generator.

In the x interval above 0.1 the data are slightly below the TWOGAM generator prediction and very close to the GRV model prediction. Any of the components used in TWOGAM can be responsible for this access. Further studies are needed to solve this uncertainty.

The proposed method for the photon structure function study has been demonstrated as being consistent. The model dependent systematic error shown by this procedure is larger than estimated by the unfolding procedure and better reflects our knowledge of the process. Only better modelling which can arise from some new physical constraints on the models can reduce such an error.

7 Acknowledgements

We are greatly indebted to our technical collaborators and to the funding agencies for their support in building and operating the DELPHI detector, and to the members of the CERN SL Division for the excellent performance of the LEP collider.

References

[1] PLUTO Collab., Ch. Berger et al., Z.Phys. **C26**, (1984) 353;
Phys. Lett. **B149**, (1984) 421;
Nucl. Phys. **B281**, (1987) 356.

[2] JADE Collab., W. Bartel et al., Z.Phys. **C24**, (1984) 231.

[3] TASSO Collab., H. Althoff et. al., Z.Phys. **C31** (1986) 527.

[4] CELLO Coll., H.-J. Behrend et al., Phys. Lett. **B126**, (1983) 391.

[5] TPC/2γ Coll., A. Aihara et al., Phys. Rev. Lett. **58**,(1987) 97
TPC/2γ Coll., A. Aihara et al., Phys. Rev. **54** 41 (1985) 736.

[6] TPC/2γ Coll A. Aihara et al., Z.Phys. **C34** (1987) 1.

[7] AMY Collab., R. Sasaki et al., Phys. Lett. **B252** (1990) 491;
S.K. Sahu et al., Phys. Lett. **B346** (1995) 208.

[8] TOPAZ Collab., K. Muramatsu et al., Phys. Lett. **B332** (1994) 478.

[9] OPAL Collab., R. Akers et al., Z.Phys. **C61** (1994) 199.

[10] DELPHI Coll., P. Abreu et al. Z.Phys. **C69** (1996) 223.

[11] OPAL Coll., K. Ackerstaff et al., Z.Phys. **C74** (1997) 33.

[12] OPAL Coll., K. Ackerstaff et al., Phys. Lett. **B411** (1997) 387.

[13] OPAL Coll., K. Ackerstaff et al., Phys. Lett. **B412** (1997) 225.

[14] OPAL Coll., G. Abbiendi et al., Eur. Phys. J. **C18** (2000) 15.

[15] L3 Coll., M. Acciarri et al., Phys. Lett. **B436** (1998) 403.

[16] L3 Coll., M. Acciarri et al., Phys. Lett. **B447** (1999) 147.

[17] L3 Coll., M. Acciarri et al., Phys. Let. **B483** (2000) 373.

[18] ALEPH Coll., R. Barate et al., Phys. Lett. **B458** (1999) 152.

[19] M. Drees and R.M.Godbole, J. Phys. **G21** (1995) 1559.

[20] L.E. Gordon and J.K. Storrow, Z.Phys. **C52** (1992) 307.

[21] M. Gluck, E. Reya and A. Vogt, Phys. Rev. **D45** (1992) 3986.

[22] H. Abramovicz, K. Charchula and A. Levy, Phys. Lett. **B269** (1991) 458.

[23] G.A. Schuler and T. Sjostrand, Z. Phys. **C68** (1995) 607.

[24] OPAL Coll., Jan A. Lauber, Proc. of the 28th Int. Conf on High Energy Physics,
World Scientific Publising Co. Pte. Ltd., (1996) 725.

[25] DELPHI Coll., Igor Tyapkin, Proc. of the 28th Int. Conf on High Energy Physics, World Scientific Publising Co. Pte. Ltd., (1996) 729.

[26] S. Nova, A. Olshevsky, T. Todorov, DELPHI-90-35 (unpublished).

[27] Humboldt University, D-10099 Berlin, FRG.

[28] T. Sjöstrand, Comp. Phys. Comm. **82** (1994) 74.

[29] G. Marchesini, B.R. Webber, G. Abbiendi, I.G. Knowles, M.H. Seymour and L. Stanco, Computer Phys. Comm. **67** (1992) 465.

[30] DELPHI Coll. , P. Aarnio et al., Nucl. Instr. and Meth., **A303** (1991), 233.

[31] DELPHI Coll., P.Abreu et al., Phys. Lett. **B342** (1995) 402.

[32] V.N. Baier et al., Phys. Rep. **78** (1981) 293.

[33] H. Plothow-Besch, PDFLIB : A Library of all available Parton Density Functions of the Nucleon, the Pion and the Photon and the corresponding α_s calculations, CERN-PPE-92-123.

[34] L. E. Gordon and J.K. Storrow, Z.Phys. **C56** (1992) 307.

[35] J.J.Sakurai and D. Schildknecht, Phys. Lett. **40B** (1972) 121; Phys. Lett. **41B** (1972) 489.

[36] V. Blobel, In Proceedings of the CERN School of Computing, Aiguablava, Spain, (1984), CERN 85-09.

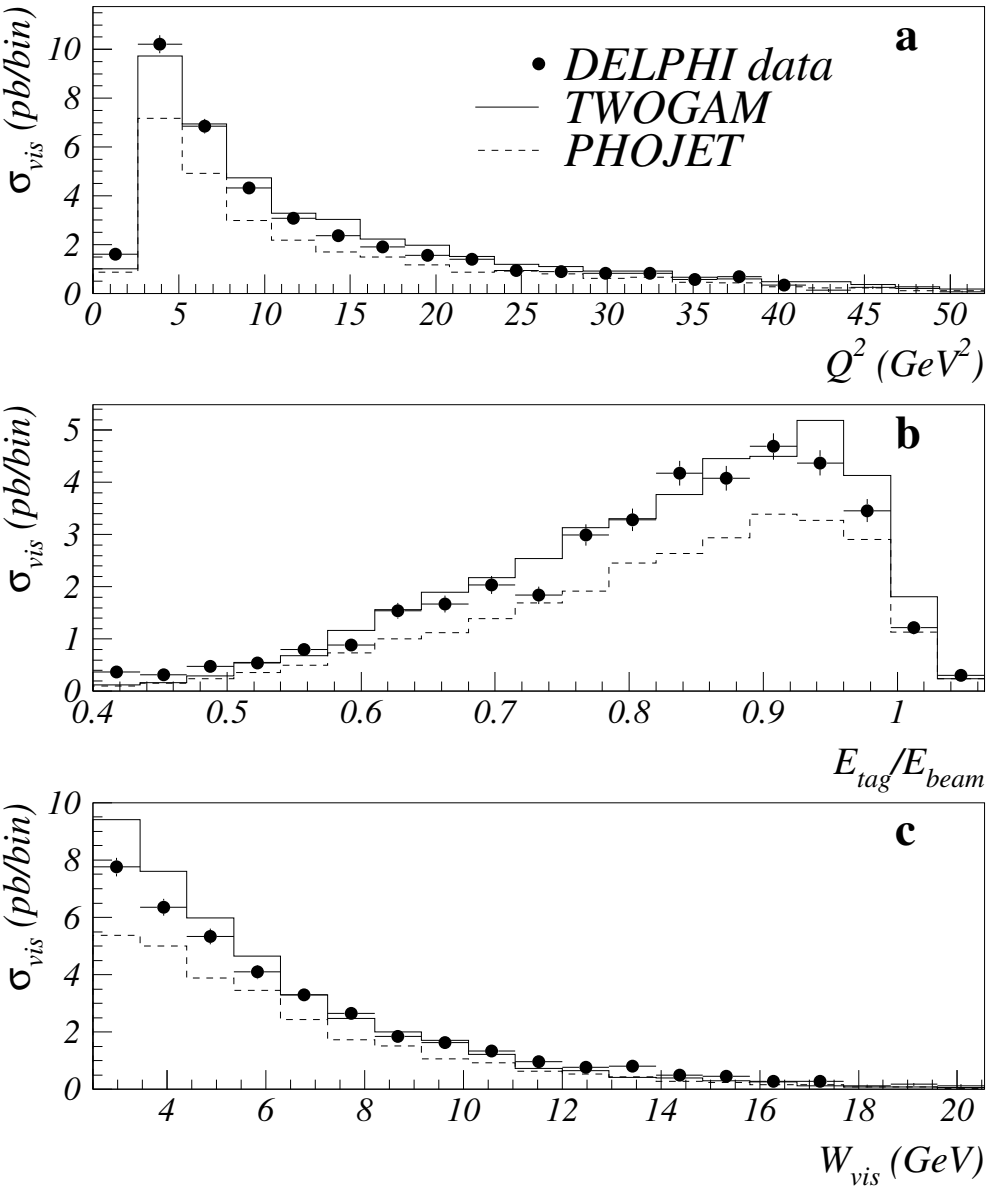

Figure 2: Comparison between data and Monte Carlo predictions for the sample with $< Q^2 >$=12.7 GeV^2: a) Q^2, b) tagging energy, c) invariant mass. Points are data and the lines show the Monte Carlo predictions from TWOGAM (solid line) and PHOJET (dashed line).

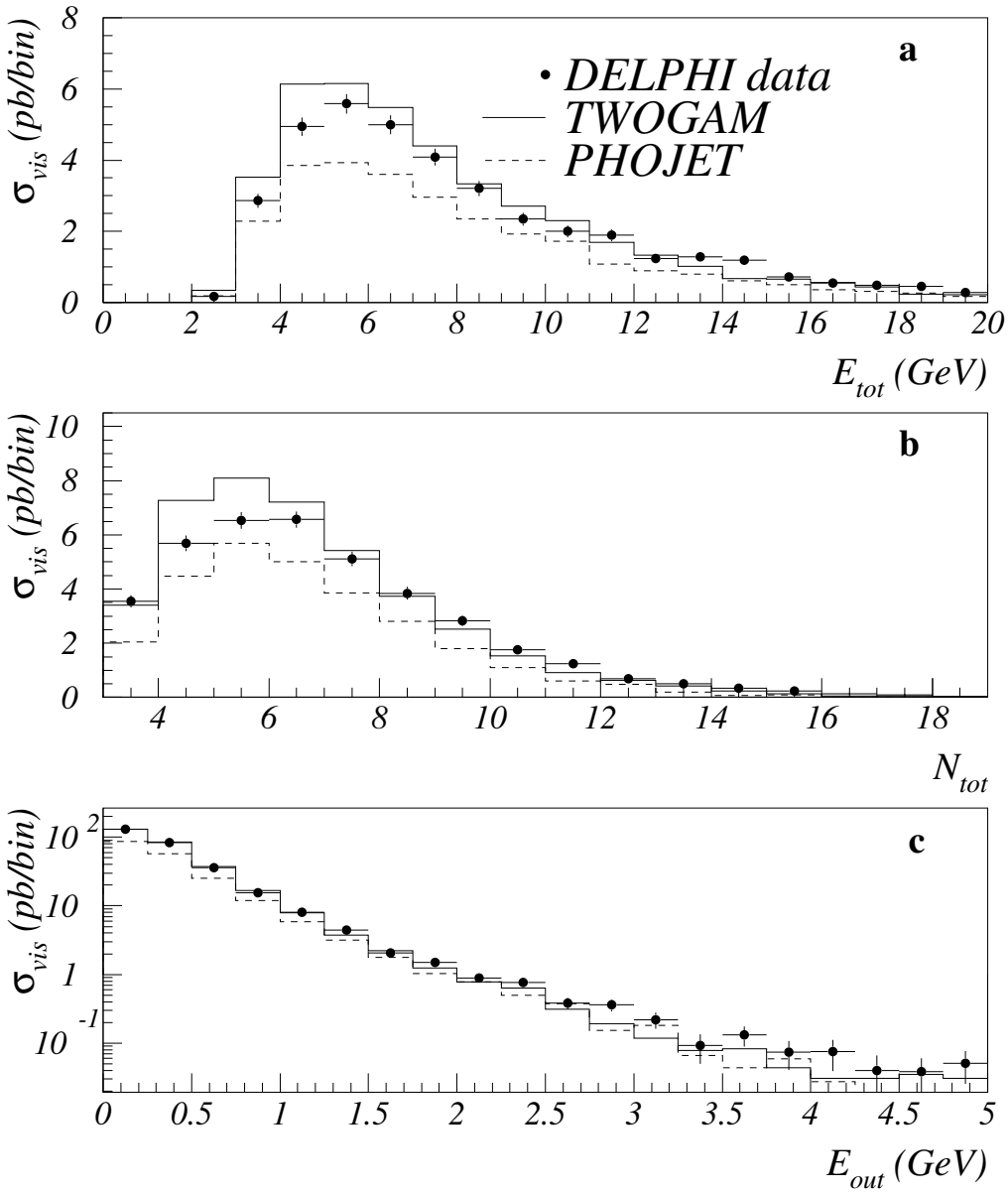

Figure 3: Comparison between data and Monte Carlo predictions for the sample with $< Q^2 >$=12.7 GeV^2: a) total energy of hadronic system, b) total number of particles, c) transverse component of hadronic energy out of plane of tagged particle . Points are data and the lines show the Monte Carlo predictions from TWOGAM (solid line) and PHOJET (dashed line).

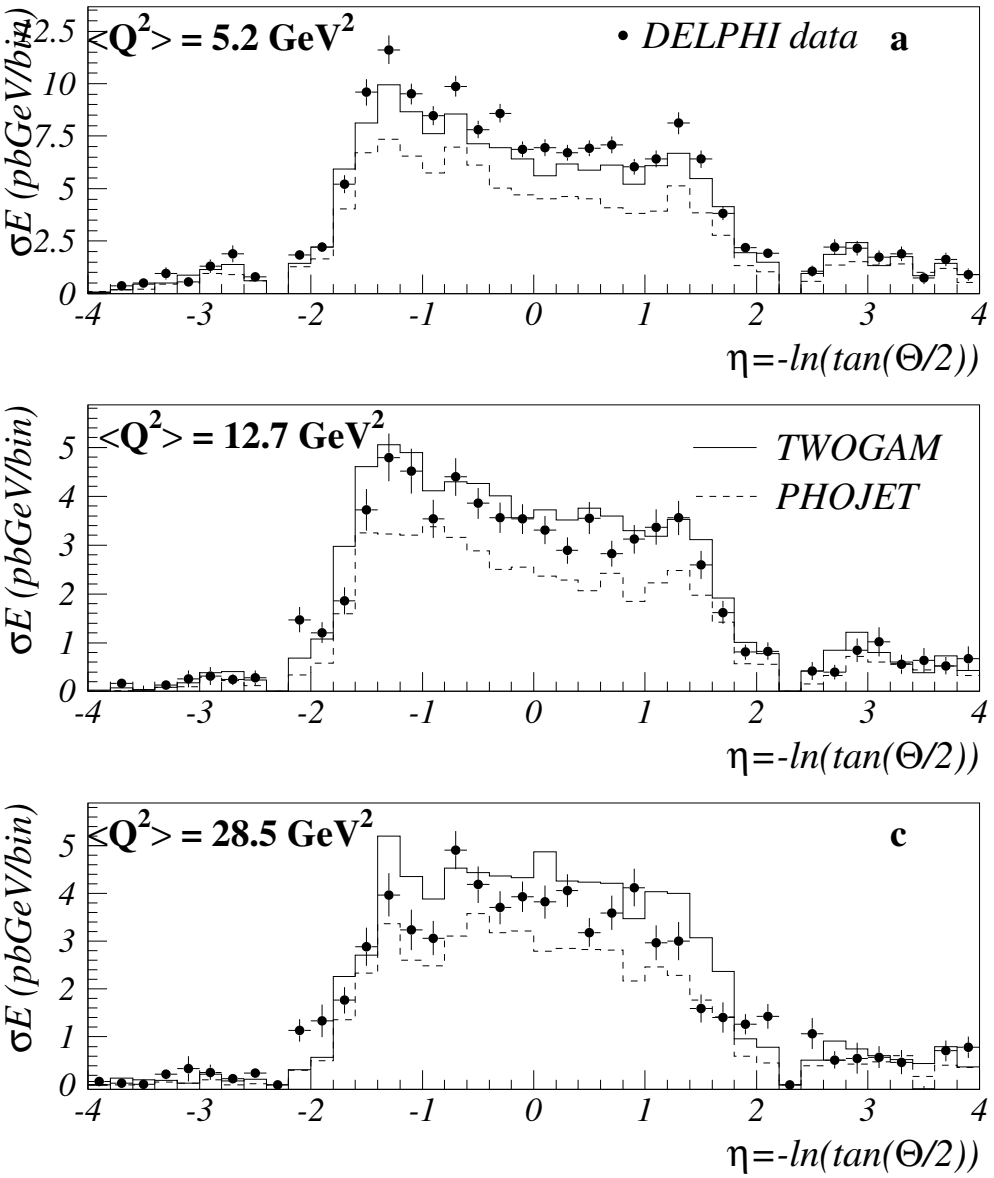

Figure 4: Comparison of hadronic energy flow for data and Monte Carlo prediction in the pseudorapidity scale for the samples in the different Q^2 regions. Points are data and the line shows the TWOGAM Monte Carlo predictions.

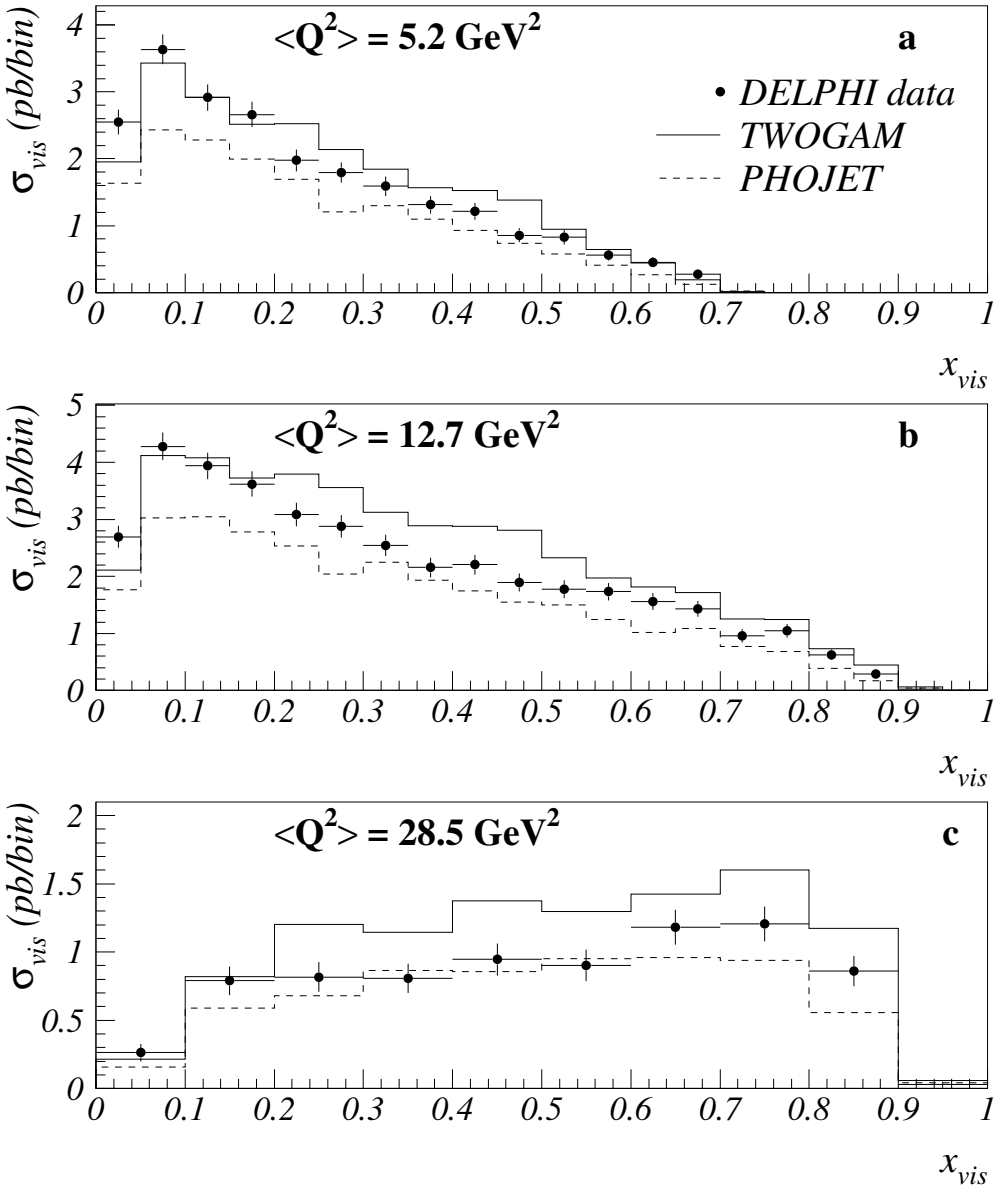

Figure 5: Comparison between data and Monte Carlo prediction for the samples in the different Q^2 regions. Points are the data and the lines show the Monte Carlo predictions from TWOGAM (solid line), PHOJET (dashed line).

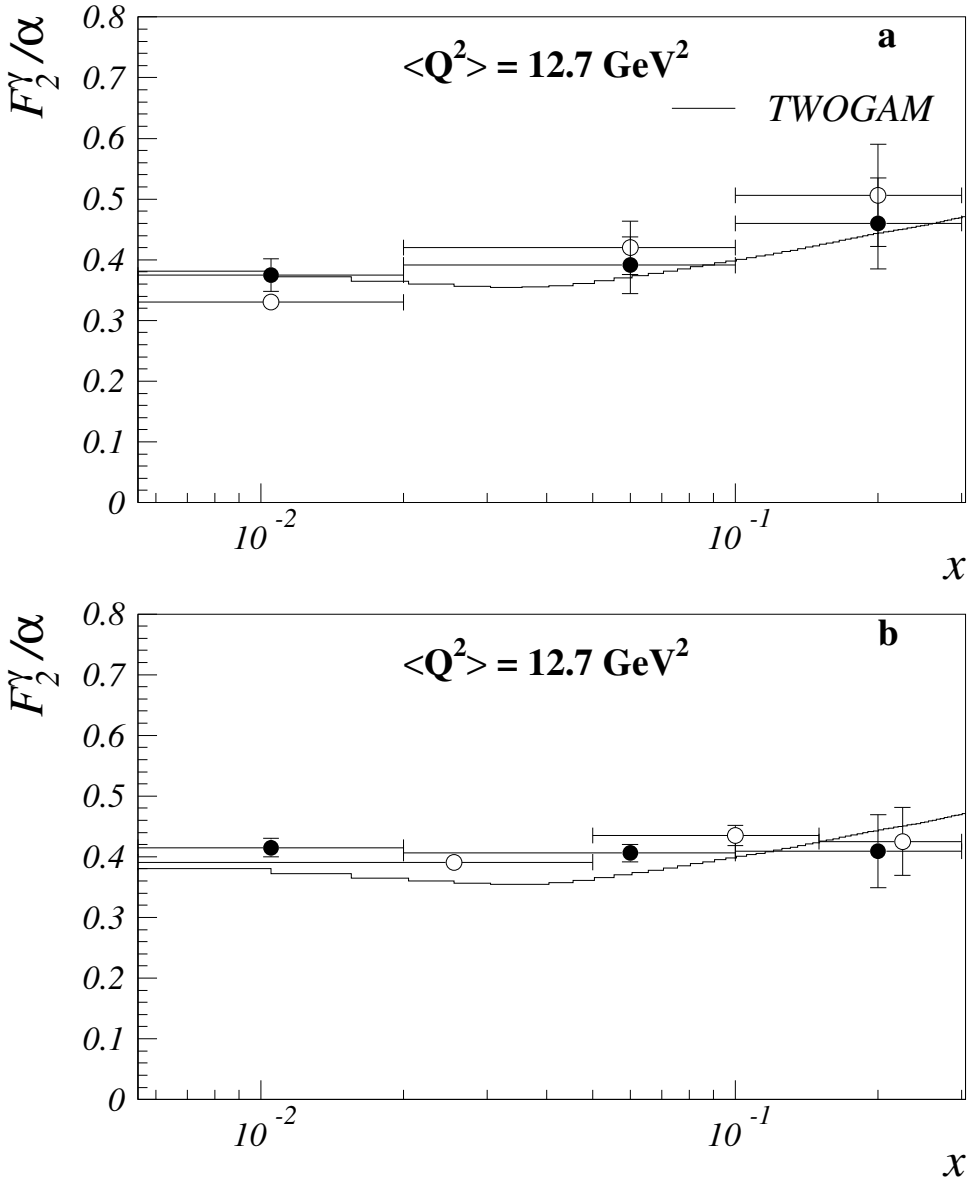

Figure 6: Test of MINUIT based procedure (a) and unfolding (b). Open circles- fit with the Monte Carlo sample treated as a sum of three components. Black dots - the complete MINUIT fitting procedure. b) The results of unfolding procedure in different x-bins.

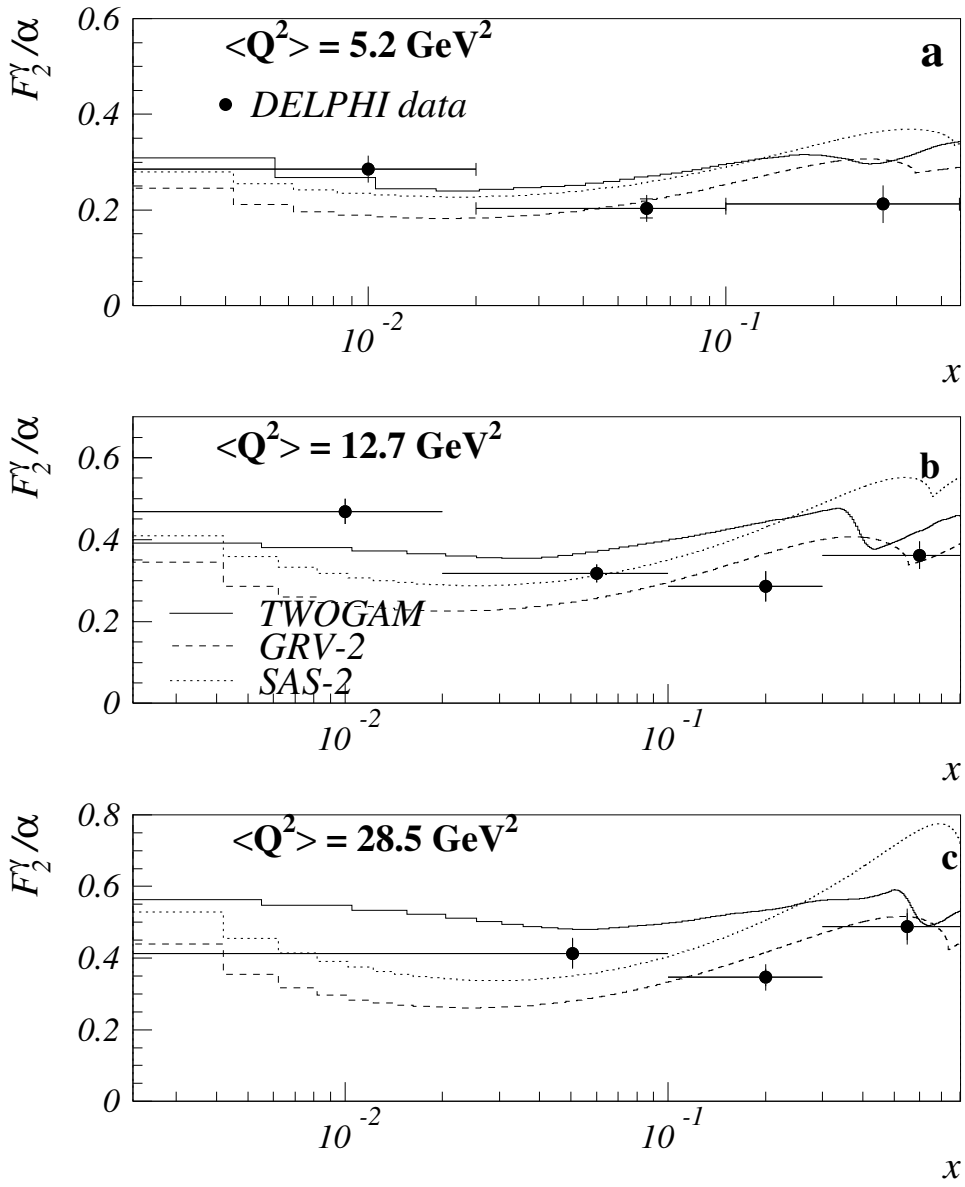

Figure 7: The measured F_2^γ at different $< Q^2 >$ as a function of x. Error bars show total errors. The data are compared with the predictions of TWOGAM program, GRV-Set2 and SaS-2d models.

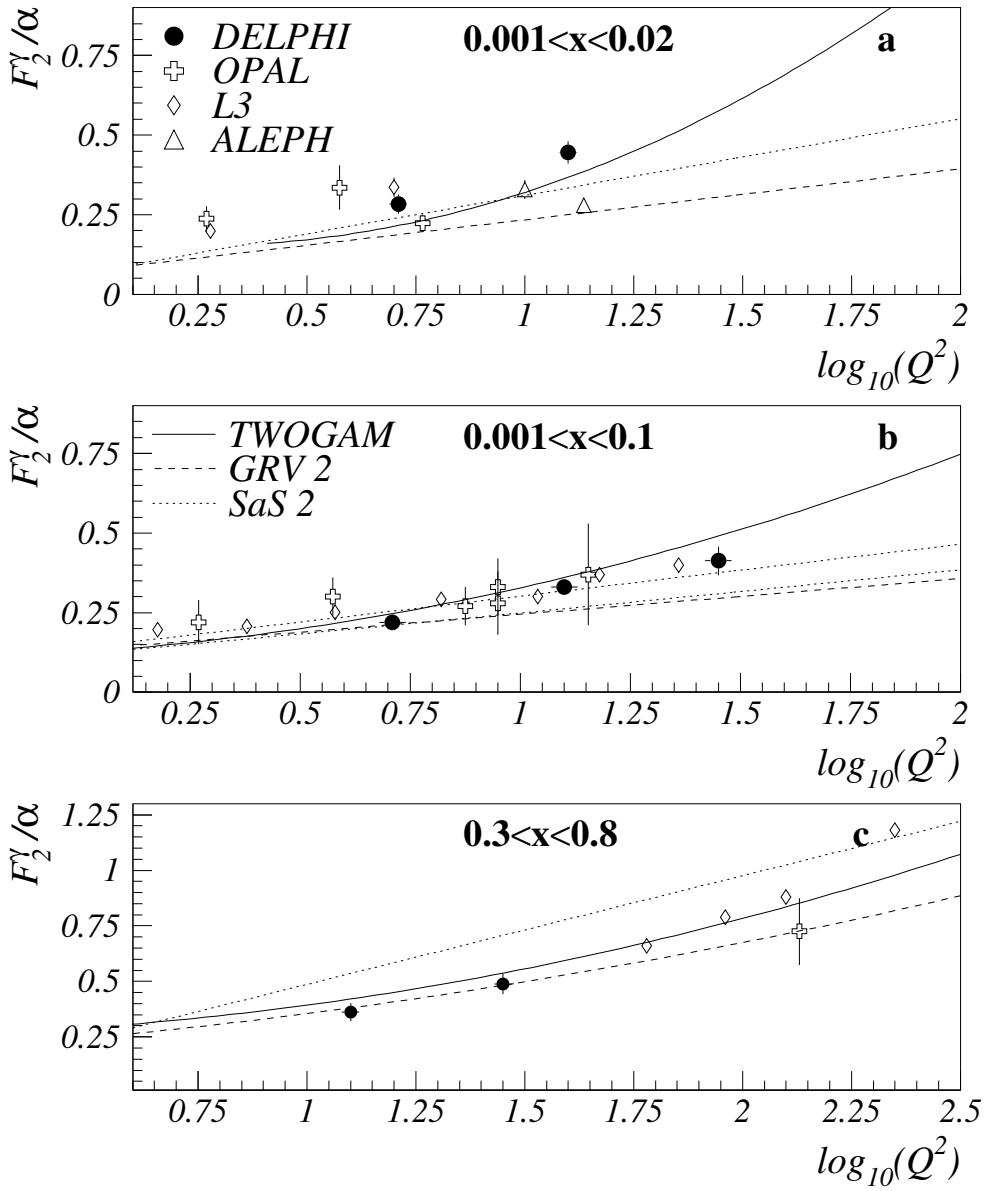

Figure 8: The measured F_2^γ in the different x intervals as a function of $< Q^2 >$ compared with predictions of TWOGAM, GRV-Set2 and SaS-2d. The statistical and systematic errors are added in quadrature. Some results from other LEP experiments are shown for the comparison.